Supporting Information

A high-temperature dielectric process as a probe of large-scale silica filler structure in simplified industrial nanocomposites

Guilhem P. Baeza,[1,2,3] Julian Oberdisse,[1,2] Angel Alegria,[3] Marc Couty,[4] and Anne-Caroline Genix[1,2*]

[1] *Université Montpellier 2, Laboratoire Charles Coulomb UMR 5221, F-34095, Montpellier, France*

[2] *CNRS, Laboratoire Charles Coulomb UMR 5221, F-34095, Montpellier, France*

[3] *Manufacture Française des Pneumatiques MICHELIN, Site de Ladoux, 23 place des Carmes Déchaux, F-63040 Clermont-Ferrand, Cedex 9, France*

[4] *Departamento de Física de Materiales y Centro de Física de Materiales CSIC-UPV/EHU, Universidad del País Vasco UPV/EHU, Paseo Manuel de Lardizabal 5, E-20018 San Sebastian, Spain*

This document gives complementary thermogravimetric results related to the water content, and shows dielectric data with detailed fit contributions for the SB-silica nanocomposites.

1. Thermogravimetric analysis (TGA)

The silica volume fractions in the nanocomposites reported here have been measured by thermogravimetric analysis (Mettler Toledo) using a first ramp at 30 K/min from 25 to 550 °C under nitrogen, followed by a second ramp at 20 K/min from 550 to 750 °C under air. From the plot of sample weight versus temperature, the silica weight fraction $\Phi_{si,w}$ remaining after thermal decomposition of the polymer and water loss was determined. The silica volume fraction $\Phi_{si,v}$ in nanocomposites was determined by mass conservation according to

$$\Phi_{si,v} = \frac{d_{SB}\Phi_{si,w}}{d_{si}\left(1-\Phi_{si,w}\right)+d_{SB}\Phi_{si,w}} \quad \text{(S1)}$$

where d_{SB} = 0.94 g.cm^{-3} and d_{si} = 2.31 g.cm^{-3} are the densities of the polymer and silica, respectively. Due to close density values between water and polymer, the small weight loss associated to water is taken into account within the polymer fraction in eq S1.

Independent measurements of the water content in the nanocomposites have been performed by TGA (Q500, TA Instruments). The sample weight loss associated with water was obtained after a ramp at 3 K/min up to 120°C followed by a 1 hour isotherm. The water content varied from 0.1 to 1.8%w for the matrix and the 21.1%v-coumpound, respectively, as determined from the plateau value. Thus, the water amount at 120°C is negligible in agreement with 0.1%w reported in ref [1], justifying the term "post-drying". The isotherms are shown in Figure S1.

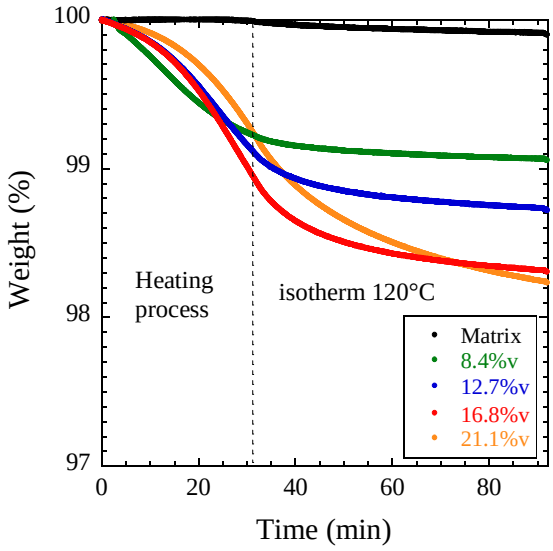

Figure S1: Thermogravimetric measurements to obtain the water content in the matrix and nanocomposites with Φ_{si} = 8.4 – 21.1%v (140 kg/mol – 50%D3).

2. Fits of the 8.4%v-nanocomposite (140 kg/mol – 50%D3)

Fit parameters associated to the fits shown in Figure 1 between 323 and 363 K for the sample with 8.4%v silica are given in Table 1. An example of fit using a single MWS-process instead of two in eq 1 is given in Figure S2. There, one can see that such an approach is not satisfactory. Two processes are needed to obtain a good description of the experimental data (ε' and ε").

Table 1: HN parameters associated to the fit functions shown in Figure 1 for temperatures between 323 and 363 K. Parameters underlined in grey have been fixed in the fit procedure, except for the MWS1 broadening which was allowed to fluctuate within 5% around its average value of 0.42.

	MWS1				MWS2			
T (K)	**Δε**	**γ**	**δ**	**log τ**	**Δε**	**γ**	**δ**	**log τ**
323	1.42	0.42	0.53	-1.14	0.42	0.55	1	0.09
333	1.49	0.42	0.53	-1.29	0.34	0.55	1	-0.54
343	1.46	0.43	0.53	-1.55	0.40	0.55	1	-1.05
353	1.45	0.43	0.53	-1.80	0.43	0.55	1	-1.50
363	1.35	0.43	0.53	-2.05	0.50	0.55	1	-1.95

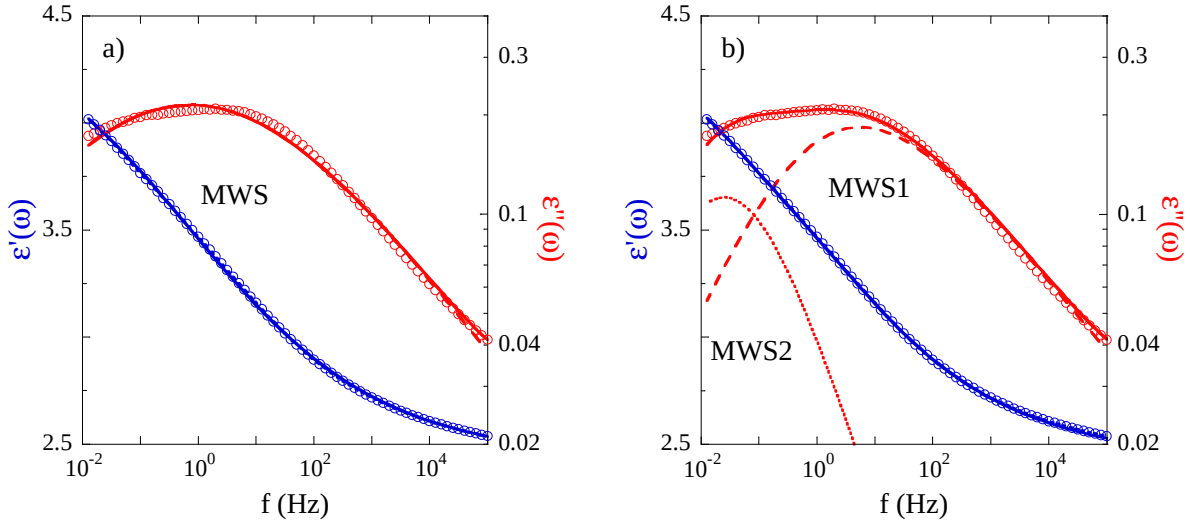

Figure S2: Frequency dependence of the real (ε') and imaginary (ε'') parts of the complex dielectric permittivity measured on a nanocomposite with 8.4%vol silica (50%D3) at T = 313 K. Solid lines through the data are fits according to eq 1 with one (a) or two processes (b). In b), the dotted and dashed lines represent the individual contributions.

3. Influence of silica fraction (140 kg/mol – 50%D3)

The necessity of two relaxation processes in order to describe the high-temperature data is shown in Figure S3 for a 21.1%vol-nanocomposite. In Figure S3 a, the dielectric loss can be crudely described by the sum of one MWS process and the dc-conductivity. Moreover, such an approach does not allow capturing the real part in the range from 10^{-2} to 10^{-1} Hz. In Figure S3 b, the sum of MWS1 and MWS2 leads to a good description of both ε' and ε''.

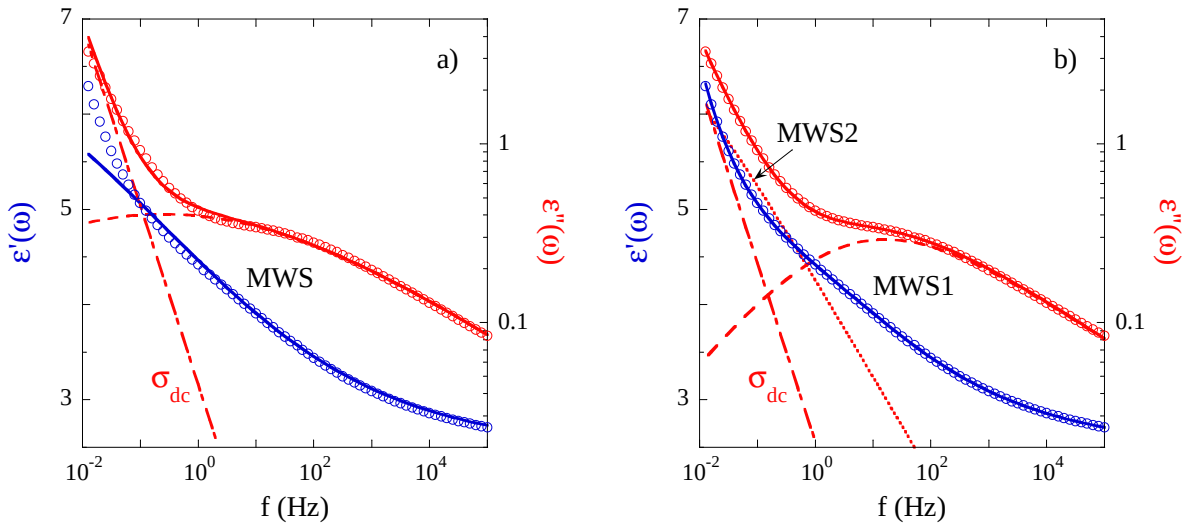

Figure S3: Frequency dependence of the real (ε') and imaginary (ε'') parts of the complex dielectric permittivity measured on a nanocomposite with 21.1%vol silica at T = 313 K. Solid lines through the data are fits according to eq 1 with dc-conductivity and one (a) or two processes (b). Broken lines represent the individual contributions.

For a better visualization of MWS1 and MWS2 processes, we use the imaginary part of the complex modulus, $M^*(\omega) = 1/\varepsilon^*(\omega) = M'(\omega) + i\,M''(\omega)$

$$M'' = \frac{\varepsilon''}{\varepsilon'^{\,2} + \varepsilon''^{\,2}} \qquad \text{(S2)}$$

Results are shown in Figure S4 for the different silica volume fractions.

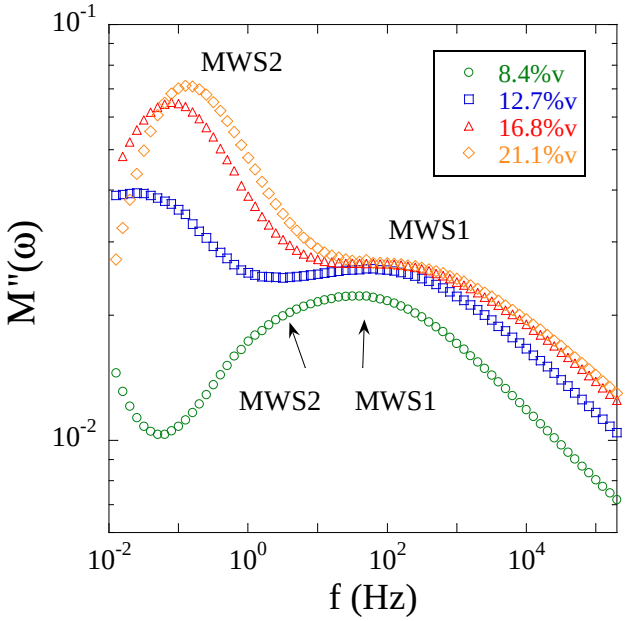

Figure S4: Dielectric loss modulus at T = 333 K for nanocomposites with Φ_{si} = 8.4 – 21.1%v.

The contributions of the fit functions shown in Figure 2 of the article are detailed in Figures S5 at 333 K.

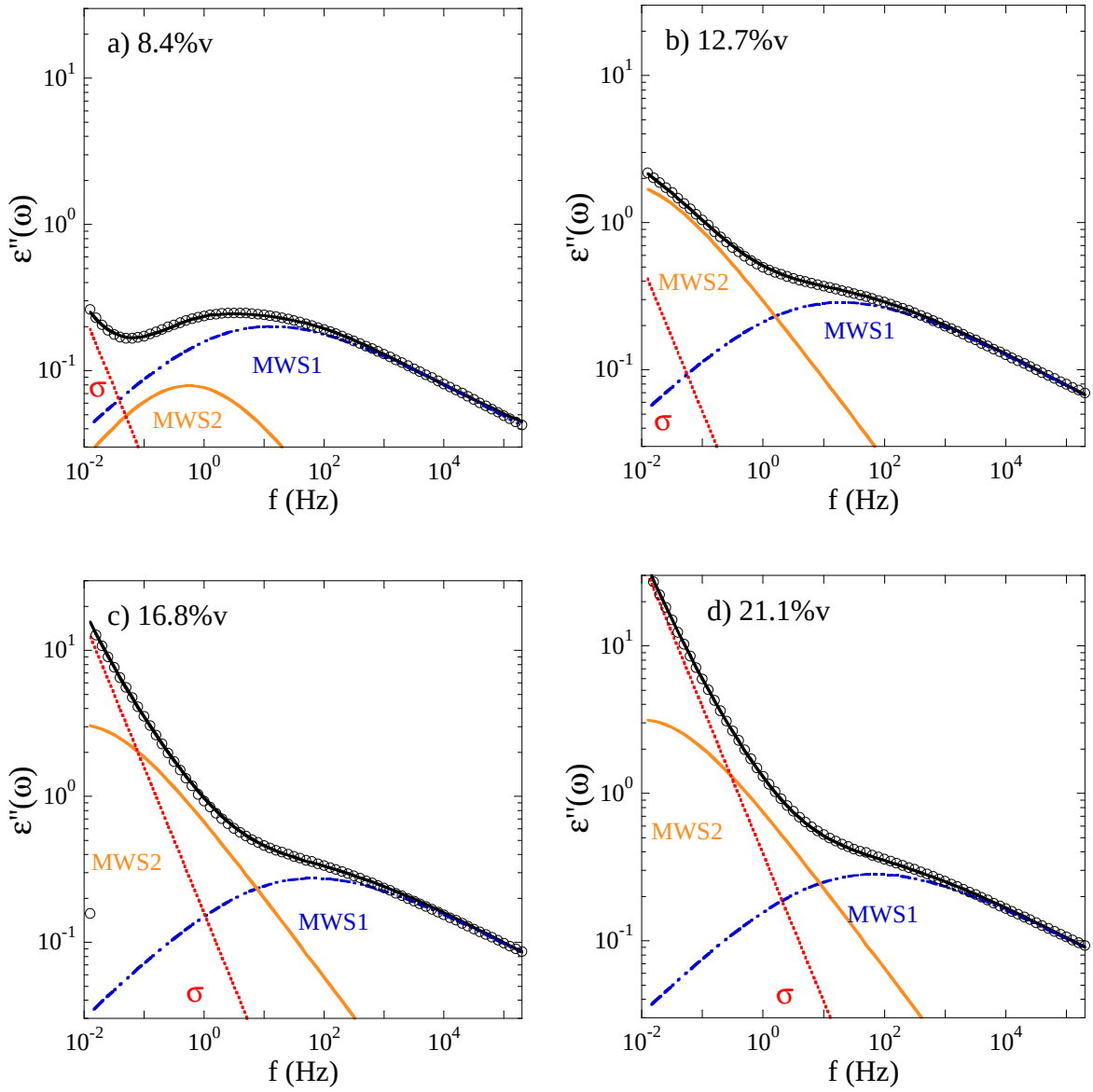

Figure S5: Dielectric loss spectra at T = 333 K for nanocomposites with Φ_{si} = 8.4 – 21.1%v from a) to d). Black lines are fits to the experimental data by means of eq 1. The dashed-dotted line stands for the MWS1 contribution, the orange line for MWS2, and the dotted line for dc-conductivity.

4. Matrix contribution in the nanocomposites

Figures S6 and S7 reproduce data given in Figures 1 and 2 with inclusion of the pure matrix data. Such a representation allows visualizing the relatively small contribution of the pure matrix in the dielectric response of the nanocomposites in the high-temperature range. There,

one can clearly see that the matrix exhibits a single ionic contribution on the low-frequency side (visible in ε’’(ω)), but no dielectric process such as in the nanocomposites. Note that all dielectric data have been normalized with respect to the high-frequency limit of the real part of the permittivity (173 K in our case). However, there may be small fluctuations on the relative positions, which can be estimated to 25% at most, and are thus negligible regarding to ε’’(ω) in log-scale.

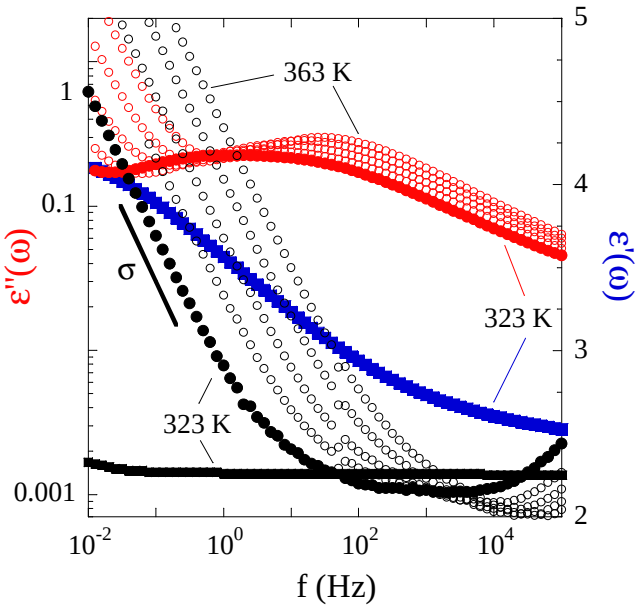

Figure S6: Frequency dependence of the imaginary (ε’’, circles) and real (ε’, squares) parts of the complex dielectric permittivity measured on a nanocomposite with 8.4%vol silica (red and blue colors) and the matrix (black) at T = 323 K. Additional data for ε’’(ω) at T = 333 up to 363 K each 10 K are also shown (empty symbols). The frequency dependence (ω^{-1}) of the ionic conductivity is highlighted by a black segment.

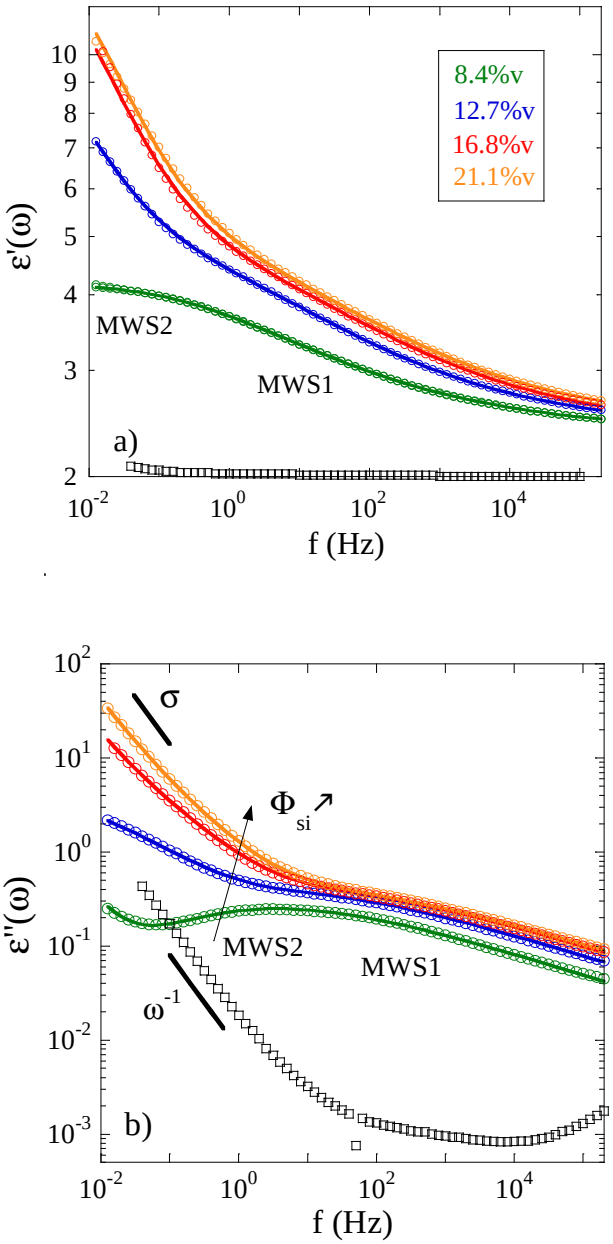

Figure S7: Dielectric spectra at 333 K for nanocomposites with Φ_{si} = 8.4, 12.7, 16.8 and 21.1%vol (circles, from bottom to top). a) Real and b) imaginary permittivity data. Solid lines are fits to the experimental data by means of eq 1. The frequency dependence (ω^{-1}) of the ionic conductivity is highlighted by black segments in b). Results for the pure matrix (squares) are given for comparison.

Reference:

1. J. Otegui, G. A. Schwartz, S. Cerveny, J. Colmenero, J. Loichen and S. Westermann, *Macromolecules*, 2013, **46**, 2407-2416.